Optically induced density depletion of the two-dimensional electron system in $GaAs/Al_xGa_{1-x}As$ heterojunctions

M. Hayne, A. Usher, and A. S. Plaut
Department of Physics, University of Exeter, Stocker Road, Exeter EX4 4QL, United Kingdom

K. Ploog
Paul Drude Institut für Festkörperelectronik, Hausvogteiplatz 5-7, D-10117 Berlin, Federal Republic of Germany

(Received 5 July 1994)

We report measurements of optically induced density depletion of the two-dimensional electron system formed at the interface of a $GaAs/Al_xGa_{1-x}As$ heterojunction with a δ-doped layer of Be acceptors in the GaAs 250 Å from the interface. Our measurements show that at low laser power the depletion effect is controlled by the recombination of two-dimensional electrons with photoexcited holes that have become bound to the Be acceptors. The point at which all the Be acceptors in the sample have been neutralized by photoexcited holes is indicated by the sudden appearance of free holes in the GaAs, which then control the density depletion in the high-power regime. We present a comprehensive dynamic model of the depletion effect that includes both regimes, and calculate the densities and mobilities of the carriers involved in the process.

I. INTRODUCTION

Recently photoluminescence experiments have been used to study the two-dimensional electron system (2DES) in the fractional quantum Hall effect and magnetically induced Wigner solid regimes.[1,2] In some of these experiments a modified structure is used in which the observed recombination is between the 2DES and holes bound to Be acceptors in a δ-doped layer a fixed distance from the interface.[3] Since the bound-hole energy is well defined, the resulting photoluminescence spectrum is determined by the energy spectrum of the recombining electrons. An important property of these samples is that continuous illumination with laser light of energy greater than the $Al_xGa_{1-x}As$ band gap results in nonpersistent reduction of the 2DES density.[4] Electrostatically, this effect is caused by charge compensation of the ionized donors in the $Al_xGa_{1-x}As$ by the photoexcited electrons.[4] The first dynamic model of the effect came from the Raman studies of Richards, Fasol, and Ploog [hereafter referred to as the Richards, Fasol, and Ploog (RFP) model].[5] In this model, the density depletion is determined by the time for an electron to tunnel through into the 2DES. Photoexcitation creates electron-hole pairs in the $Al_xGa_{1-x}As$, where the electrons are confined by the barrier potential before they eventually tunnel into the 2DES. In contrast, the holes are quickly swept into the GaAs, where they are captured by the Be acceptors (Fig. 1). Concentration reduction occurs because the photocreated holes recombine rapidly with the electrons in the 2DES, while the tunneling of photoexcited electrons from the $Al_xGa_{1-x}As$ is relatively slow. This model was first proposed to explain a laser-induced density-depletion effect observed in $GaAs/Al_xGa_{1-x}As$ quantum wells, where the quantum well traps the holes near the 2DES so that they are available for recombination.[6]

II. EXPERIMENTAL RESULTS

We have used photoluminescence and low-field Hall measurements to study the variation of the 2DES density with illumination from an Argon-ion laser. Our measurements were conducted using a silica fiber to illuminate the Hall bar sample uniformly and to collect the luminescence. The sample (details of which can be found in Table I) was cooled to temperatures <0.3 K, depending on the laser power used, in magnetic fields of up to 17 T. We have found that the density-depletion effect is not

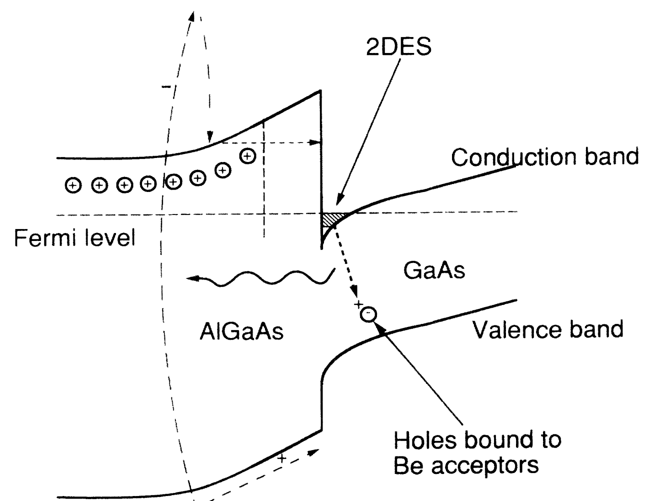

FIG. 1. Schematic diagram of a $GaAs/Al_xGa_{1-x}As$ heterojunction with a δ-doped layer of Be acceptors 250 Å from the interface. The observed recombination and the mechanism for density depletion at low-incident laser power are also shown (see text for details).

 ©1994 The American Physical Society

TABLE I. Details of the sample parameters used in the model. Additional sample parameters that are not required for the calculation are also given.

Sample model parameters	
Bohr radius of hole bound to acceptor[a], a_0	50.8 Å
Spacer layer thickness, d	175 Å
Thickness of doped $Al_xGa_{1-x}As$ region, d_1	525 Å
Permittivity, ε	$12.56\varepsilon_0$[b]
Effective mass of 2D electrons, m^*_{2d}	$0.067m_0$[c]
Effective mass of electrons in $Al_xGa_{1-x}As$[d], m^*_e	$0.092m_0$[c]
Effective mass of free holes in GaAs, m^*_{fh}	$0.4m_0$[c]
Maximum 2DES density, n^0_{2d}	6×10^{11} cm^{-2}
Density of acceptors in the δ-doped layer, N_a	2.5×10^{10} cm^{-2}
Acceptor saturation power, P_{sat}	10 mW
2DES to bound-hole recombination time[e], τ_b	110 ns
Aluminum concentration fraction, x	0.3
Additional sample parameters	
Density of donors in $Al_xGa_{1-x}As$	2×10^{17} cm^{-3}
Distance of Be acceptors from interface	250 Å
Thickness of GaAs buffer region	600 Å

[a]A. Baldereschi and N. O. Lipari, Phys. Rev. B 8, 2697 (1973).
[b]ε_0 is the permittivity of free space.
[c]m_0 is the free-electron mass.
[d]N. Chand, T. Henderson, J. Klem, W. T. Masselink, R. Fischer, Y. C. Chan, and H. Morkoç, Phys. Rev. B 30, 4481 (1984).
[e]See Ref. 16.

only dependent on the electron tunneling time, but that it is determined largely by the action of the photoexcited holes.

Since the holes with which the two-dimensional (2D) electrons recombine are bound to acceptors that are in a δ layer, the zero magnetic-field recombination spectrum should be a direct measure of the zero-field 2D density of states. Localization of the holes removes the requirement for wave-vector conservation in the transition, and the δ layer ensures that the hole contribution to the 2DES-to-neutral-acceptor recombination energy is well defined. Thus, the 2DES concentration can be determined from the luminescence width by

$$n_{2d}=\frac{m^*_{2d}(E_f-E_b)}{\pi\hbar^2}, \tag{1}$$

where m^*_{2d} is the 2DES effective mass, E_f is the Fermi energy of the 2DES, and E_b is the bottom of the 2DES subband. In practice, the presence of disorder and a Fermi-edge singularity[7] means that the zero-field luminescence line is not the "top-hat" shape that we would expect for the 2D density of states, and the Fermi energy and bottom of the subband are not directly identifiable from the data. We have taken E_f and E_b to be equal to the high- and low-energy edges, respectively, of the recombination line at half the maximum intensity (Fig. 2). Figure 3 shows the Fermi edge (circles), the peak position (squares), and the bottom of the 2DES subband (triangles) at zero magnetic field as a function of laser power. At all powers the Fermi energy remains constant, while the peak position and the bottom of the 2DES subband increase in energy with laser power up to about 10 mW, above which there is no further change. This implies a monotonic decrease in the 2DES density below 10 mW, and no change above this point.

We also expect the disorder-induced line broadening to decrease as the laser power is increased as a result of two mechanisms. These are screening of the Si donors by the photoexcited electrons in the $Al_xGa_{1-x}As$, and neutralizing of the Be acceptors. In order to use the linewidth to see changes in the electron concentration, we must also try to take this into consideration. To do this we use the high-energy half-width as a measure of the amount of disorder felt by the 2DES. Since the position of the high-energy edge of the line (the Fermi energy) is independent of power, we need only look at changes in the peak position to measure the change in disorder (Fig. 3, inset). This shows a monotonic decrease in the disorder contribution to the linewidth, up to about 10 mW, where there is no further change. We believe that this corresponds to the point where all the Be acceptors have been neutralized by photoexcited holes and, therefore, that the acceptors are the dominant source of the disorder felt by the 2DES. Since both the total linewidth and the broadening due to disorder show a monotonic decrease up to a power of 10 mW, and then saturate beyond this power, we can conclude that the 2DES concentration has the same behavior. However, because of the nonideal shape of the zero-field luminescence spectra, a quantitative measurement of the 2DES density from these data will probably

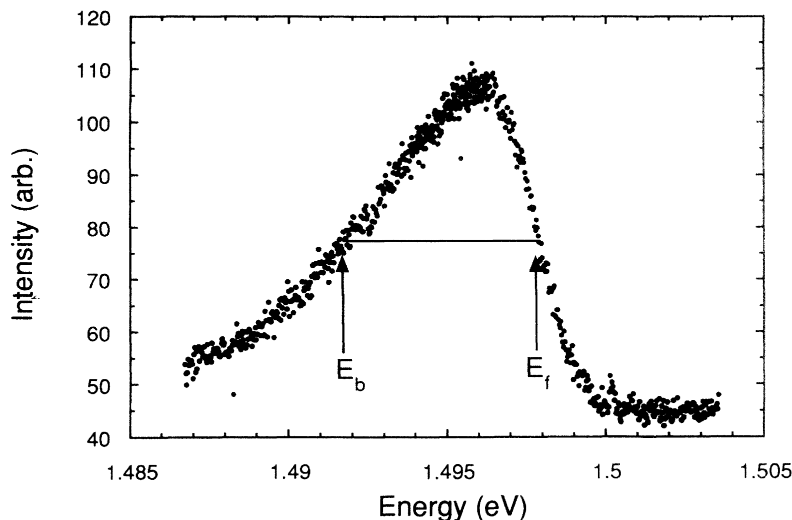

FIG. 2. 2DES to bound-hole recombination line at zero magnetic field for a nominal laser power of 0.6 mW. Here, as elsewhere, the laser power is the power emitted from the laser multiplied by the absorption of the neutral-density filters. The position of the Fermi energy (E_f) and bottom of the subband (E_b), as defined in the text, are also shown.

not be reliable.

A second method of determining the 2DES concentration is by studying the changes in the photoluminescence line position as a function of magnetic field.[2,8] Figure 4 shows a fan diagram at an incident laser power of 0.6 mW. There are two spectral lines, which can be identified as the first (LL0) and second (LL1) Landau levels. At 4.5 T, LL1 depopulates (filling factor $\nu=2$), and there is a corresponding shift of LL0. At about twice the field, a second shift occurs ($\nu=1$), caused by enhancement of the g factor as the upper spin-state level is depopulated.[8] By studying the field position of these features, we have been able to measure the electron density as a function of incident power (Fig. 5, triangles).

We have also used low-field Hall measurements to determine the 2DES concentration in the sample. Unfortunately, it is not always possible to determine the concentration by observation of minima in the Shubnikov–de Haas oscillations because with high illumination levels transport features are washed out by parallel conduction from photocreated electrons in the $Al_xGa_{1-x}As$. Hall measurements will be unaffected as long as the conductance of the 2D electrons is very much greater than the conductance of the bulk electrons, which is true at very low fields (< 1 T). Figure 5 (circles) shows the variation of the density as measured from the Hall voltage, assuming a single type of carrier. The Hall density shows the same power dependence as the 2DES density measured from the optical features below about 10 mW. However, above 10 mW the Hall density shows a sudden increase, such that it rapidly exceeds the density at the lowest laser-illumination levels. This is in direct contradiction to the zero-field width data, taken in conjunction with these measurements, which indicate that the 2DES density remains at a minimum value at these powers. We conclude that the change in the Hall voltage is due to the breakdown of the condition that the bulk conductivity is very much less than the 2DES conductivity, resulting from the sudden introduction of *free holes* in the GaAs. (The free electrons in the $Al_xGa_{1-x}As$ remain relatively unimportant because of their low mobility, as discussed in Sec. V below.) In the model of RFP, the

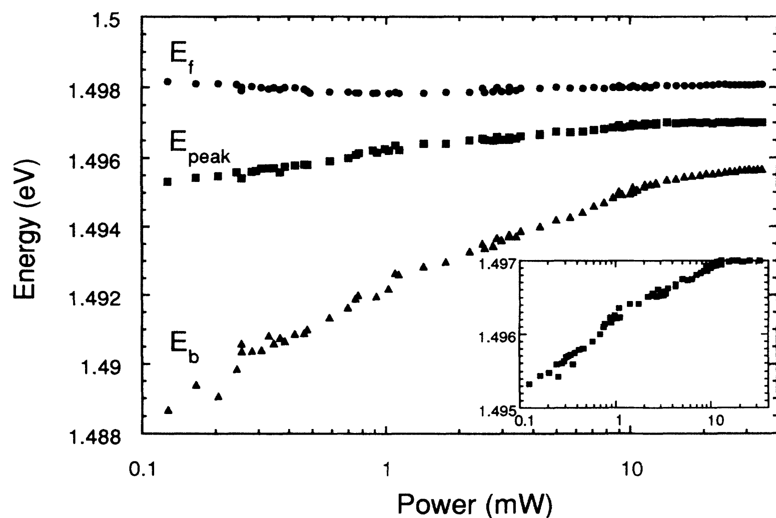

FIG. 3. The Fermi edge E_f (circles), peak position E_{peak} (squares), and bottom of the 2DES subband E_b (triangles) at zero magnetic field plotted as a function of laser power. The inset shows the peak position in more detail.

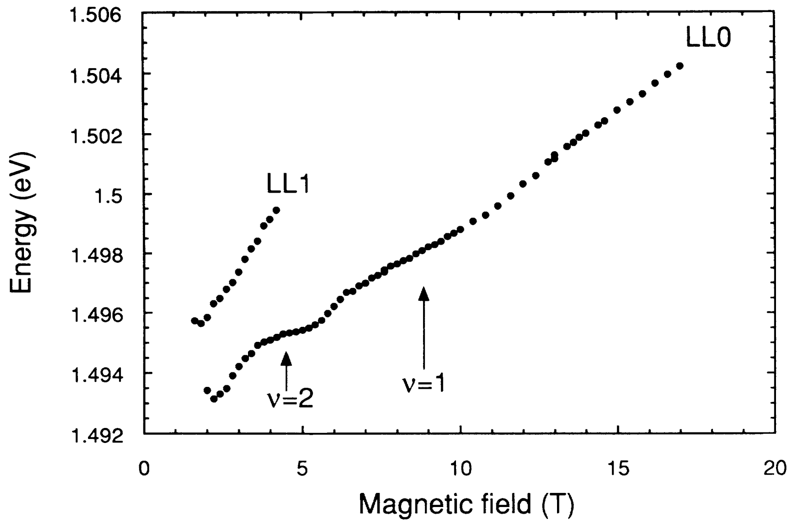

FIG. 4. Fan diagram at a power of 0.6 mW and a 2DES density of 2.2×10^{11} cm^{-2}. Landau levels are not resolved below 2 T. The positions of filling factors $\nu=2$ and $\nu=1$ are also shown.

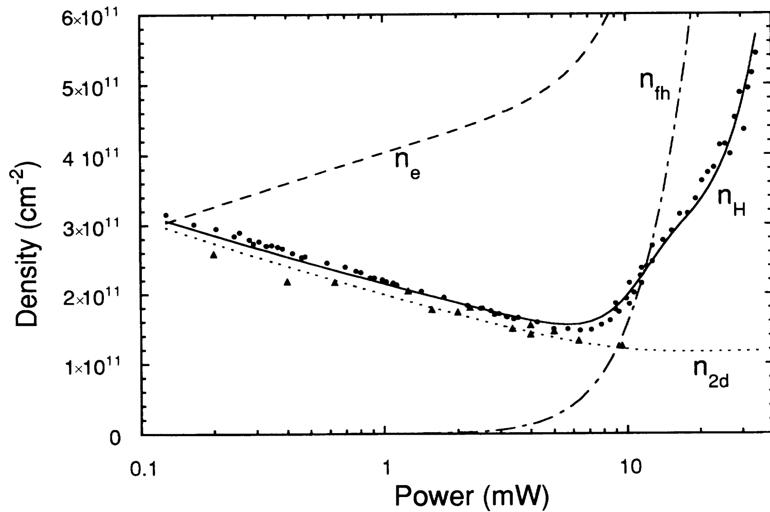

FIG. 5. Measured and calculated carrier densities in the sample under continuous illumination. The Hall density (n_H) is given by circles (experimental) and the solid line (fit). The 2DES density (n_{2d}) is given by triangles (measured from optical features) and the dotted line (calculated). The calculated densities of the electrons in the $Al_xGa_{1-x}As$ (n_e) and free holes in the GaAs (n_{fh}) are given by dashed and dot-dashed lines, respectively.

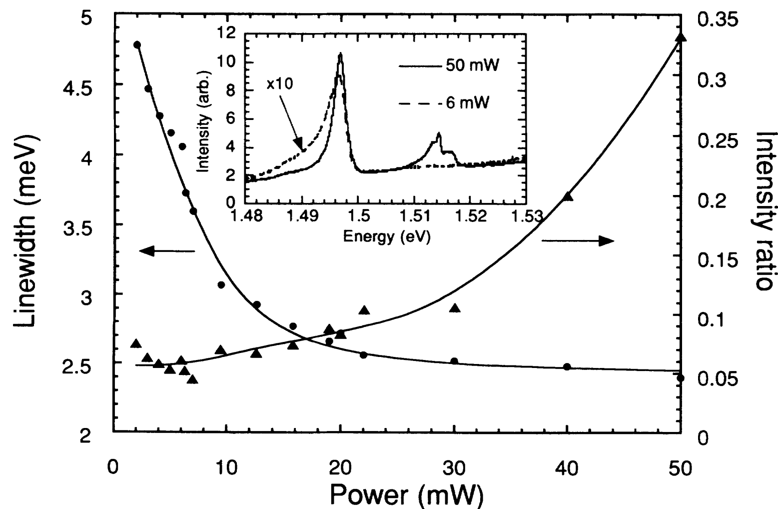

FIG. 6. Demonstration that the appearance of the free holes is coincident with saturation of the 2DES density. The circles are the full width at half-maximum of the 2DES-to-bound-hole recombination line, and the triangles are the ratio of the free-hole recombination intensity to the bound-hole recombination intensity. In both cases, the solid lines are a guide to the eye. The inset shows recombination spectra at 0.6 mW (dashed line, intensity $\times10$) and 50 mW (solid line).

density depletion in these samples is a result of electrons from the 2DES recombining with the holes bound to Be acceptors that are close to the interface. There are, however, a limited number of Be acceptors in the δ-doped layer, and when all of the Be acceptors have been neutralized by photoexcited holes, any excess holes will be free to move in the GaAs. The sudden presence of free holes in the sample is confirmed by the appearance of 2DES-to-free-hole and bulk-GaAs recombination lines in the luminescence spectra. Figure 6 shows the ratio of the free-hole to bound-hole recombination intensity as a function of laser power. Also shown is the width of the 2DES-to-bound-hole recombination line as a function of laser power. The free-hole recombination intensity is negligible until the linewidth reaches its minimum value, when it rapidly increases indicating that saturation of the density-depletion effect occurs at the same time as the appearance of the free holes.

III. DENSITY-DEPLETION MODEL

Previous explanations of the laser-induced density depletion in these samples have concentrated on the role of the photocreated electrons in this process, but our results show that the role of the photocreated holes is equally important. The model of RFP assumed that the effect is determined only by the rate at which the electrons depleted from the 2DES can be replaced by tunneling of photoexcited electrons from the $Al_xGa_{1-x}As$. This model works well at low power, when the density of bound holes is small, but breaks down at high powers when all the Be acceptors have captured holes. We have developed a dynamic model of the density-depletion effect, which includes not only the accumulation of electrons in the $Al_xGa_{1-x}As$, but also the trapping of holes in the Be δ-doped layer, and at high powers the appearance of free holes in the GaAs.

Our dynamic model includes the fact that the photoexcited holes remain bound to the Be acceptors for a finite time before they recombine, allowing the possibility that all of the Be acceptors in the δ-doped layer will have captured holes. This contrasts with the model of RFP, which assumes that the 2DES-to-bound-hole recombination is infinitely fast. Charge conservation in the sample requires that the total carrier charge must be equal to the charge due to the ionized impurities

$$N_d d_1 - N_a = n_{2d} + n_e - n_{\rm bh} - n_{\rm fh} , \tag{2}$$

where N_d is the 3D density of ionized donors in the $Al_xGa_{1-x}As$, d_1 is the thickness of the doped $Al_xGa_{1-x}As$ region, N_a is the density of acceptors in the δ-doped layer, n_e is the density of electrons in the $Al_xGa_{1-x}As$, $n_{\rm bh}$ is the density of holes bound to the Be acceptors, and $n_{\rm fh}$ is the density of free holes in the GaAs. (Note that throughout this discussion all densities are areal densities unless otherwise stated.) In the dark, but after the saturation of the persistent photoconductivity effect,[9] the only carriers will be those in the 2DES, which will have a maximum density $n_{2d}^0 = N_d d_1 - N_a$. Since this value is easily determined from transport measurements, we substitute it into Eq. (2). We also consider the effect of electron-hole pairs excited in the GaAs by the laser illumination. In this process the photoexcited electrons are swept into the 2DES, contributing to n_{2d} rather than n_e. The holes will remain in the bulk of the GaAs, and since they are indistinguishable from the holes that are created in the $Al_xGa_{1-x}As$ and then swept into the GaAs, they will contribute to $n_{\rm bh}$ and $n_{\rm fh}$ as usual. The laser illumination will create $\eta_{\rm eh}$ electron-hole pairs per unit area per second, which we can relate to the carrier densities using the carrier lifetimes. Equation (2) now becomes

$$n_{2d}^0 = n_{2d} + \alpha\eta_{\rm eh}\tau_t - f\tau_b - (\eta_{\rm eh} - f)\tau_f , \tag{3}$$

which can be rewritten as

$$n_{2d} = f(\tau_b - \tau_f) + \eta_{\rm eh}(\tau_f - \alpha\tau_t) + n_{2d}^0 .$$

Here τ_b is the 2DES to bound-hole recombination time, τ_f is the 2DES to free-hole recombination time, τ_t is the inverse of the rate at which the electrons in the $Al_xGa_{1-x}As$ tunnel into the 2DES, α is the proportion of the electron-hole pairs that are created in the $Al_xGa_{1-x}As$, and $f = f(\eta_{\rm eh})$ is a function which gives the density of photoexcited holes that bind to the Be acceptors per second. It can be seen in Fig. 5 that the Hall carrier density and the 2DES density measured from features in the optics are approximately equal below 10 mW, except for a few points at very low power. (This discrepancy is probably due to a sample with inhomogeneous density, with the parts of the sample at the lowest density, where $n_{\rm bh}$ is the largest, giving rise to the strongest luminescence.) We can also see from Fig. 6 that the 2DES to free-hole recombination is negligible at low power. Both of these observations imply that all of the photoexcited holes must bind to Be acceptors in this regime. Conversely, at high power when all the Be acceptors are neutralized, the number of photoexcited holes that bind to the Be acceptors per second must be equal to N_a/τ_b. We, therefore, choose an empirical function for f that has these properties given by

$$f = \frac{N_a}{\tau_b}\tanh\left[\frac{\eta_{\rm eh}\tau_b}{N_a}\right] . \tag{4}$$

This is equal to $\eta_{\rm eh}$ at low power and equal to N_a/τ_b at high power as required. Furthermore, the rapid changeover between the two regimes is well described by this function.

We now consider τ_t. We assume that the barrier exists in the spacer layer, which contains no charge, so we can model it as a triangular potential, with a width that is equal to the spacer thickness d, and a slope that is equal to the electric field at the interface, which changes with the concentration of the 2DES. Thus,

$$V(z) = \frac{e^2 n_{2d} z}{\varepsilon} , \tag{5}$$

where ε is the permittivity and $z=0$ corresponds to the bottom of the barrier. An electron at $z=0$ (i.e., in the doped part of the $Al_xGa_{1-x}As$) will remain there for a time

$$\tau_t = A \exp\left[\frac{4e}{3\hbar}\left[\frac{2d^3 m_e^* n_{2d}}{\varepsilon}\right]^{1/2}\right], \tag{6}$$

where m_e^* is the effective mass of the electrons in the $Al_xGa_{1-x}As$ and A is a constant. If we choose a parabolic barrier with the electric field matched at the interface and equal to zero in the bulk $Al_xGa_{1-x}As$ at a distance d from the interface, we obtain the same result except for a factor of $3/(4\sqrt{2})$ in the exponential. We relate η_{eh} to the incident power by noting that at the power P_{sat} at which all of the acceptors have just become neutralized, $\eta_{eh} = N_a/\tau_b$, thereby avoiding the uncertainty involved in estimating the laser power density absorbed by the sample.

In the low power limit, where all the photoexcited holes are trapped by the Be acceptors $f = \eta_{eh}$, and provided that we assume $\alpha\tau_t \gg \tau_b$, Eq. (3) reduces to

$$n_{2d}^0 = n_{2d} + \alpha\eta_{eh}\tau_t , \tag{7}$$

which is equivalent to the expression used by RFP. At high illumination levels, when all the Be acceptors have trapped holes $f = N_a/\tau_b$, so any further change in density is determined by the free holes, via the difference between τ_f and $\alpha\tau_t$. When the 2DES density reaches a minimum these times become equal, thus we substitute n_{min} into Eq. (6) to find τ_f. In order to compare our model with the Hall density data of Fig. 5, we also need to calculate the mobilities of both the 2D and 3D carriers in the sample. This is discussed in the following section.

IV. CARRIER MOBILITIES

For clarity we have used simple analytical expressions to calculate the 2D and 3D mobilities. In the 3D case we start from the Brooks-Herring result for scattering of a carrier with energy E and wave vector $\mathbf{k}$ by ionized impurities[10]

$$\frac{1}{\tau^{ii}(E,\mathbf{k})} = \frac{N_{ii}e^4}{16\sqrt{2m}\,\pi\varepsilon^2}E^{-3/2}\left[\ln(1+b) - \frac{b}{1+b}\right], \tag{8}$$

where

$$b = \left[\frac{2|\mathbf{k}|}{\beta}\right]^2, \tag{9}$$

N_{ii} is the 3D density of ionized impurities, β is the inverse screening length, m is the carrier mass, and τ_{ii} is the scattering time. For a low-temperature degenerate gas all the scattering occurs at the Fermi energy, thus $E = E_f$, $\mathbf{k} = \mathbf{k}_f$, and β is the 3D Thomas-Fermi screening parameter, yielding an expression for the mobility,

$$\mu^{ii} = \frac{24\pi^3\varepsilon^2 n}{N_{ii}m^2}\left[\frac{\hbar}{e}\right]^3\left[\ln(1+b) - \frac{b}{1+b}\right]^{-1}. \tag{10}$$

The mobility for electrons in the $Al_xGa_{1-x}As$ caused by ionized impurities (μ_e^{ii}) is found by substituting $N_{ii} = N_d = (n_{2d}^0 + N_a)/d_1$, and $n = n_e/d_1 = \alpha\eta_{eh}\tau_t/d_1$. It is noteworthy that N_d is not equal to the total density of donors in the $Al_xGa_{1-x}As$, but rather to the density of deep donor-related defects (DX centers).[11] At low temperatures, the cloud of photocreated electrons in the $Al_xGa_{1-x}As$ will bind to the shallow donors in the $Al_xGa_{1-x}As$, but not to the DX centers, this being the property that is responsible for the persistent photoconductivity effect.[9] We also include alloy disorder scattering of the electrons in the $Al_xGa_{1-x}As$, modeled by randomly situated potential wells of size ΔE,[12]

$$\mu_e^{al} = \frac{8}{3\sqrt{2\pi}}\frac{e\hbar^4 N_{al}}{E_f^{1/2} m_e^{*5/2} x(1-x)(\Delta E)^2}, \tag{11}$$

where N_{al} is the density of aluminum sites. There is at present no consensus as to the value ΔE should take,[13] so we include it as an adjustable parameter. The total inverse mobility for the electrons in the $Al_xGa_{1-x}As$ is found by using Matthiessen's rule

$$\frac{1}{\mu_e} = \frac{1}{\mu_e^{al}} + \frac{1}{\mu_e^{ii}}. \tag{12}$$

The ionized acceptor contribution to the free-hole mobility, μ_{fh}^{ia} is also found from Eq. (10), where $n = n_{fh} = (\eta_{eh} - f)\tau_f$ and $N_{ii} = N_{ia} = N_a - f\tau_b$ is the number of acceptors that have not been neutralized by photoexcited holes. However, since $N_a - f\tau_b$ tends to zero at high laser power, we also include the scattering due to neutral acceptors, given by the usual expression for the mobility derived assuming a hydrogenlike state for a hole bound to the acceptor[14]

$$\mu_{fh}^{na} = \frac{e}{20\hbar a_0 (N_{na})^{3/2}}, \tag{13}$$

where a_0 is the Bohr radius of the bound hole, and $N_{na} = f\tau_b$ is the number of neutral acceptors in the GaAs. As above, the total hole mobility (μ_{fh}) is found using Matthiessen's rule.

Finally, we turn to the 2DES mobility. We have explicitly considered three possible scattering mechanisms: the ionized donors in the $Al_xGa_{1-x}As$, the ionized acceptors in the GaAs, and the neutral acceptors in the GaAs. Again, it is convenient for us to use analytical expressions for the 2D mobilities, thus for the ionized impurity scattering we follow Lee *et al.*[15] The mobility arising from ionized acceptor scattering is given by

$$\mu_{2d}^{ia} = \frac{8\pi\hbar^3\varepsilon^2 k_{f2d}^2 I(B_{2d})}{e^3 m_{2d}^{*2} N_{ia}}, \tag{14}$$

where $I(B_{2d})$ is the scattering integral, which can be approximated to

$$\frac{1}{I(B_{2d})} = 1.26B_{2d}^2 + 2.21B_{2d} + 0.74, \tag{15}$$

and $B_{2d} = 1/b$ given by Eq. (9) for the two-dimensional case. The scattering by remote impurities is given by[15]

$$\mu_{2d}^{ri} = \frac{64\pi\hbar^3\varepsilon^2 k_{f2d}}{e^3 m_{2d}^2 N_d (1/L_0^2 - 1/L_1^2)}, \tag{16}$$

where L_0 and L_1 are the average distances of the 2DES

to the nearest and furthest edges of the doped region, respectively.

The 2DES mobility will be determined by Eq. (14) at low power, since the scattering will be dominated by the charged acceptors in the proximity of the 2DES. In Sec. II, we briefly discussed the screening of the ionized donors by the photoexcited electrons in the $Al_xGa_{1-x}As$. At high power the dense gas of photoexcited electrons in the $Al_xGa_{1-x}As$ will be very efficient at smoothing out the fluctuations in the potential due to the ionized donors. This means that ionized donor scattering of the 2DES is not significant in either regime, and can be neglected. In addition, the acceptors become neutralized by the photoexcited holes at high power. However, they still determine the 2DES mobility via neutral impurity scattering. There must be wave-function overlap between the electrons in the 2DES and the neutral acceptors in order for luminescence to occur, so the neutral acceptors which limit the mobility of the holes in the GaAs at high laser power will also scatter the 2D electrons. In order to model this effect, we note that Eq. (13) is dependent only on the density of the neutral impurities; thus, although it would be inappropriate to apply it to the 2DES directly, due to the small wave-function overlap between the 2DES and the neutral acceptors, we use this expression multiplied by a fitting parameter $r_{\rm na}$.

V. DISCUSSION

In Fig. 5 we show the fit to the Hall density data given by

$$n_H = \frac{(\mu_{\rm fh} n_{\rm fh} + \mu_e n_e + \mu_{2d} n_{2d})^2}{\mu_{\rm fh}^2 n_{\rm fh} - \mu_e^2 n_e - \mu_{2d}^2 n_{2d}} , \quad (17)$$

using the densities and mobilities of the three different charge carriers calculated as described above. We also show the densities of the electrons in the $Al_xGa_{1-x}As$ (dashed line), the holes in the GaAs (dot-dashed line), and the electrons in the 2DES (dotted line). A summary of the values taken for the fixed parameters is given in Table I. For the fitting parameters we find $A' = \alpha A = 5.26$ ns, $r_{\rm na} = 13.0$, and $\Delta E = 1.42$ eV, the last of which falls within the range of values (0–1.6 eV) quoted in the literature.[13] It can be seen that the calculated Hall density data are in very good agreement with the experimental data over the entire power range, compelling evidence that our model for the density depletion is correct. We also note that the calculated 2DES density agrees equally well with the density as measured optically over most of the laser-power range. (The small discrepancy at low power has been explained in Sec. III above.) This is further strong evidence that our depletion model is correct; our fit is to the Hall data, not to the measurement of the density via features in the optics. At low power (< 10 mW), the number of free holes is very small and since the mobility of the electrons in the $Al_xGa_{1-x}As$ is low, the Hall density is a measure of the 2DES density to a fair approximation. In the narrow range of powers between 10 and 20 mW, the behavior of the Hall density is more complex, yet the agreement between the experimental data and the fit remains excellent. In this regime the sudden rise in the density of free holes results in the rapid increase in the Hall density. A secondary effect is a rise in the 2DES mobility [Fig. 7(a)] due to the changeover from ionized impurity scattering to neutral impurity scattering [Fig. 7(b)], causing the kink that appears in both the experimental Hall data and the fit. At the highest powers, the mobility and the density of the 2DES remain unchanged, and the contribution to the Hall density from the free holes becomes increasingly important. In the high-power regime (> 10 mW), there is also a rapid rise in the number of electrons in the $Al_xGa_{1-x}As$ coincident with the appearance of free holes. This must occur to preserve charge conservation. As the density of bound holes becomes constant, the increase in the number of free holes must be matched by an increase in the number of electrons, either in the 2DES, or as is the case, in the $Al_xGa_{1-x}As$. In fact, the density of electrons in the $Al_xGa_{1-x}As$ (and holes in the GaAs) is proportional to the incident power in this regime. This is because n_{2d}, and therefore τ_t, are constant, and is in contrast with the low-power region where τ_t is varying. However, the sudden change in the Hall density is almost entirely due to the appearance of the free holes in the GaAs, with only a very small contribution from the low mobility electrons in the $Al_xGa_{1-x}As$ [Fig. 7(a)].

Once all the Be acceptors have captured holes then any further change in the 2DES density results from the difference between τ_f and $\alpha\tau_t$. If $\tau_f < \alpha\tau_t$ at $P_{\rm sat}$, then the 2DES density will continue to drop, but if $\tau_f > \alpha\tau_t$ at $P_{\rm sat}$, then it should actually start to rise again. It is interesting to note that in this sample n_{2d} stays constant from this point, implying that $\tau_f = \alpha\tau_t$ at $P_{\rm sat}$. As the power is increased, the 2DES density will always change in such a way as to make τ_f eventually equal to $\alpha\tau_t$, but there is no reason why this should happen close to $P_{\rm sat}$. In addition, at low power where Eq. (3) reduces to Eq. (7), the density depletion is also independent of τ_b. Furthermore, if we double τ_b, which is equivalent to moving the acceptors further away, we find that $P_{\rm sat}$ halves. This is simply because each hole remains bound to an acceptor for twice as long, so you need generate only half as many to neutralize all the acceptors. Thus, since the density depletion is independent of τ_b in both regimes, it is also independent of the distance of the δ-doped layer from the interface, in agreement with experimental results.[16] This result will break down when $\tau_f \gg \alpha\tau_t$, for example, when recombination to free holes does not occur. In this case the 2DES density will always start to rise at $P_{\rm sat}$.

Finally, we discuss the implications of our model with regard to the design of samples with higher mobilities and lower densities. In both the low- and high-power regimes, it is the acceptors that limit the 2DES mobility, so an increase in mobility can simply be achieved by moving the acceptors further away from the interface, and thereby reducing the wave-function overlap. As mentioned above, this does not usually affect the 2DES density depletion. The limiting case of this would be to remove them completely, corresponding to a depletion effect governed entirely by recombination to free holes.[17] How-

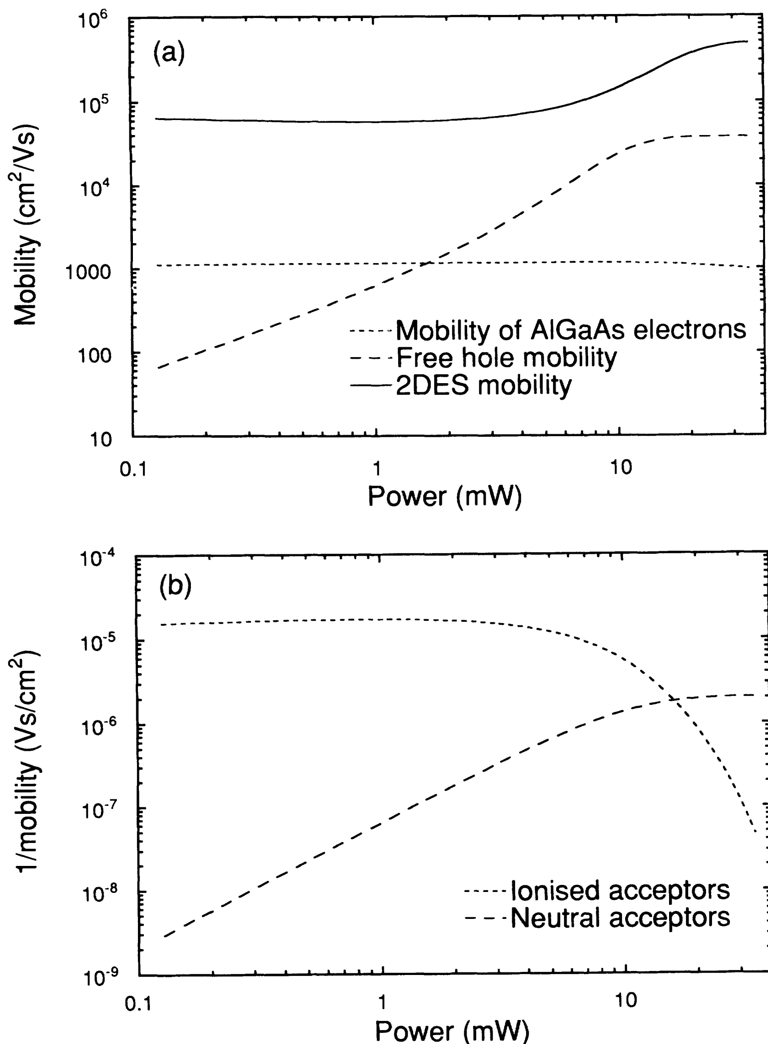

FIG. 7. (a) Calculated mobilities in the sample as a function of laser power. The solid line is the 2DES mobility, the dashed line is the free-hole mobility, and the dotted line is the mobility of the electrons in the $Al_xGa_{1-x}As$. (b) Relative contributions to the 2DES mobility from neutral acceptors (solid line) and ionized acceptors (dashed line).

ever, for some luminescence experiments[2,18] it is advantageous to study the 2DES-to-bound-hole recombination. For transport measurements it is necessary to avoid the region above P_{sat}, due to the large number of bulk carriers present in the sample. Since moving the acceptors further away reduces P_{sat}, such measurements will always be problematic.

We easily see that the best way to reduce the minimum 2DES density is to increase the spacer width if we substitute $n_{2d}=n_{min}$ and $\tau_f=\alpha\tau_t$ into Eq. (6) and rearrange to give

$$n_{min}=\frac{\varepsilon}{2d^3m_e^*}\left[\frac{3\hbar}{4}\ln\left[\frac{\tau_f}{\alpha A}\right]\right]^2 . \tag{18}$$

This will have two beneficial effects. First, for an overall $Al_xGa_{1-x}As$ thickness (doped layer plus spacer) of 700 Å, as is the case for this sample, only about 45% of the light from an Argon-ion laser is absorbed in the $Al_xGa_{1-x}As$.[19] Not only does this low absorption in the $Al_xGa_{1-x}As$ increase n_{min} in accordance with Eq. (18), but it makes the laser illumination inefficient by increasing unwanted absorption in the GaAs. This has important implications for low-temperature experiments where low laser-illumination powers are needed. If we double the spacer width to 350 Å, for example, we find that the proportion of light absorbed in the $Al_x\ Ga_{1-x}As$ increases to 84%. The second effect is considerably more dramatic: the minimum 2DES density has an inverse cubic dependence on the spacer width, so doubling the spacer width will reduce n_{min} by a factor of 8.

VI. CONCLUSIONS

We have studied the laser-induced 2DES density depletion in a $GaAs/Al_xGa_{1-x}As$ heterojunction with a δ layer of Be acceptors in the GaAs 250 Å from the interface. At low power the effect results from recombination to holes, which are bound to the Be acceptors. We have shown that further illumination causes the excess holes to appear as free carriers in the GaAs, which then govern the depletion effect. We have developed a comprehensive dynamic model of the density depletion, which deter-

mines the electron densities in the 2DES and the $Al_xGa_{1-x}As$, and the hole density in the GaAs. Our model is valid in both power regimes and can be used in the design of similar samples for future experiments.

ACKNOWLEDGMENT

This work was supported by the Science and Engineering Research Council, U.K.

[1] I. N. Harris, H. M. D. Davies, R. A. Ford, J. F. Ryan, A. J. Turberfield, C. T. Foxon, and J. J. Harris, Surf. Sci. **305**, 61 (1994); S. A. Brown, A. G. Davies, A. C. Lindsay, R. B. Dunford, R. G. Clark, P. E. Simmonds, H. H. Voss, J. J. Harris, and C. T. Foxon, *ibid.* **305**, 42 (1994); D. Heiman, A. Pinczuk, M. Dahl, B. S. Dennis, L. N. Pfeiffer, and K. W. West, *ibid.* **305**, 50 (1994), and references therein.

[2] I. V. Kukushkin, R. J. Haug, K. von Klitzing, and K. Ploog, Surf. Sci. **305**, 55 (1994), and references therein.

[3] I. V. Kukushkin, K. von Klitzing, K. Ploog, and V. B. Timofeev, Phys. Rev. B **40**, 7788 (1989).

[4] I. V. Kukushkin, A. S. Plaut, K. von Klitzing, and K. Ploog, Surf. Sci. **229**, 447 (1990).

[5] D. Richards, G. Fasol, and K. Ploog, Appl. Phys. Lett. **57**, 1099 (1990).

[6] A. S. Chaves, A. F. S. Penna, J. M. Worlock, G. Weimann, and W. Schlapp, Surf. Sci. **170**, 168 (1986).

[7] P. Hawrylak, Phys. Rev. B **45**, 4237 (1992).

[8] A. S. Plaut, I. K. Kukushkin, K. von Klitzing, and K. Ploog, Phys. Rev. B **42**, 5744 (1990).

[9] D. V. Lang, R. A. Logan, and M. Jaros, Phys. Rev. B **19**, 1015 (1979).

[10] D. Chattopadhyay and H. J. Queisser, Rev. Mod. Phys. **53**, 745 (1981).

[11] For review, see P. M. Mooney, J. Appl. Phys. **67**, R1 (1990).

[12] J. W. Harrison and R. J. Hauser, Phys. Rev. B **13**, 5347 (1976).

[13] A. Chandra and L. F. Eastman, J. Appl. Phys. **51**, 2699 (1980); A. Saxena and A. R. Adams, *ibid.* **58**, 2640 (1985); A. Baraldi, C. Ghezzi, A. Parisini, A. Bosacchi, and S. Franchi, Phys. Rev. B **44**, 8713 (1991).

[14] C. Erginsoy, Phys. Rev. **79**, 1013 (1950).

[15] K. Lee, M. S. Shur, T. J. Drummond, and H. Morkoç, J. Appl. Phys. **54**, 6432 (1983).

[16] I. V. Kukushkin (private communication).

[17] J. G. Michels, S. Hill, R. J. Warburton, G. M. Summers, P. Gee, J. Singleton, R. J. Nicholas, C. T. Foxon, and J. J. Harris, Surf. Sci. **305**, 33 (1994).

[18] M. K. Ellis, M. Hayne, A. Usher, A. S. Plaut, and K. Ploog, Phys. Rev. B **45**, 13 765 (1992).

[19] D. E. Aspnes, S. M. Kelso, R. A. Logan, and R. Bhat, J. Appl. Phys. **60**, 754 (1986).